EFFECTIVE TENSILE STIFFENING IN PRESTRESSED CONCRETE WALL SEGMENTS

L. CHITNUYANONDH, S. RIZKALLA, D. W. MURRAY, J. G. MacGREGOR

University of Alberta, Department of Civil Engineering,
Edmonton, Alberta T6G 2G7, Canada

SUMMARY

Concrete after cracking continues to contribute to the stiffness of structures. Hence analyses based on a "tension cut-off" assumption will tend to overestimate strains and, consequently, displacements. This paper describes a series of tests carried out on relatively large scale prestressed concrete wall segments. The specimens were loaded in tension in an attempt to simulate the conditions which would occur in thin-walled prestressed shell type secondary containment structures subjected to internal overpressures. From the results of these tests the cracking strengths were determined and related to standard split cylinder strengths. The strengths exhibited by the wall segments were considerably lower than the tensile strengths obtained from the cylinder tests.

The results of the tests were also used to determine an effective uniaxial average stress-strain curve for concrete in tension. The use of the stress-strain curve, with an elastic-plastic biaxial concrete constitutive theory in tension, allows an analyst to simulate the average strains in the post-cracking range of response of prestressed concrete wall segments. A degrading stress-strain curve is determined for each of the test specimens and a lower bound approximation is recommended on the basis of these test results. It is demonstrated that, when this curve is used as input to an elastic-plastic analysis, good correlation between predicted and experimental results can be obtained.

1. Introduction

A typical secondary containment structure associated with nuclear power plants is composed of prestressed concrete shell segments. These structures often consist of a vertical cylindrical shell with a spherical cap. Their geometry is such that the components satisfy the restrictions whereby they may be classified as "thin shells", and the classical assumptions of normals remaining straight and normal to the middle surface are considered adequate for their analysis.

In the event of extreme internal overpressures such shells would become primarily tension structures. A simple 'tension cut-off' analysis could be employed to obtain an estimate of their ultimate strength which is primarily dependent upon the reinforcement contained within the concrete. However, the extent and distribution of cracking during the progressive deterioration of the structure is likely to be grossly overestimated by a 'tension cut-off' analysis. Although the concrete may crack at specific locations, the concrete between cracks continues to contribute to the effective stiffness of the structure. Thus the post-cracking distribution of forces, and the size and distribution of cracks (and hence the leakage characteristics) are highly dependent on the effective properties of the concrete when it acts in conjunction with reinforcement after crack initiation.

The objective of this paper is to analyze the results obtained from a series of tests in which post-tensioned "wall segments" were subjected to tensile forces in order to determine the post-cracking properties of concrete. More specifically, the objective herein is to deduce from the test results an effective uniaxial stress-strain curve of concrete in tension which, when supplied as input to an elastic-plastic material model, permits the prediction of strains which are consistent with experimental observations.

2. Wall Segment Tests

The specimens for a typical wall segment test have dimensions of 31.5 x 31.5 x 10.5 inches (800 x 800 x 267 mm) and were post-tensioned with 3-6 wire grouted tendons of the BBR type in one direction with or without 4-7 wire grouted tendons in the orthogonal direction. Orthogonal layers of reinforcing steel were located close to both of the lateral faces of the specimen. The main variables in the test series were size of reinforcing bars, cover on the reinforcing, and the ratio of applied external forces. The specimens were intended to represent segments extracted from cylindrical or spherical shells forming the secondary containment structure, which is loaded primarily by tensile membrane forces.

The side view of a typical segment is shown in Fig. 1. The segments were post-tensioned shortly after casting. The tendons were then grouted and cured for at least 28 days. Control cylinders (6" x 12") were cast at the same time as the specimen in order to relate the specimen behavior to standard material test results. Material tests were carried out at the time of testing of the main specimen and consisted of compression tests to measure f'_c and split cylinder tests to measure f'_t.

Most specimens were loaded in direct tension without intentional moment. Tensile forces in the order of 550 kips (2500 Newtons) were applied to the specimens in one or both directions. The load in the vertical direction was applied by an MTS 1.2×10^6 lb. testing machine, while that in the horizontal direction was applied by pairs of 2×10^5 lb. hydraulic jacks. Fig. 2 shows the test set up. The load was transferred to the specimen through the reinforcing steel and prestressing tendons which extended beyond the perimeter of the specimen. Thus the boundary of the specimen can be considered to be equivalent to the face of an existing crack. The specimen was centered both ways in the testing machine and the distribution of forces on the reinforcing steel and tendons were measured under a nominal load. Mechanical adjustments to the coupling devices were made until the desired distribution of applied forces was achieved.

Throughout the test, measurements were taken on electrical resistance strain gages on the reinforcing steel and the concrete, and on Demec points on the concrete. Overall extension was measured with LVDT's. Cracks were identified as they formed and propagated. Crack locations and crack width measurements were recorded. A detailed description of the instrumentation and testing procedure is contained in Ref. 1. The loading was continued until the average stress in the prestressing tendons exceeded 95% of the minimum guaranteed ultimate strength. A typical segment at the termination of the test is shown in Fig. 3.

3. Method of Determining Tensile Strength

In terms of structural behavior the primary variables which govern the overall response of a section in tension are the concrete cracking strength and the rate of post-cracking degradation of the effective stiffness of the concrete. In processing the data from the test series these characteristics have been determined separately. The cracking load was determined from load-strain plots as the "intersection point" of the tangent lines to the precracking and post-cracking response. This was usually a well defined point since both precracking and post-cracking response were essentially linear.

The measured strains were determined as the average strains obtained from four 5-inch Demec gage lengths in each direction contained within a 15 x 15 inch (381 x 381 mm) square, centered on the side face of the specimen. Such measurements were taken on each face of the specimen. Since the specimen loading contained unavoidable eccentricities, the cracking strength was determined by computing the stress on a face as

$$f''_t = \frac{P_{cr}}{A_t} + \frac{M_{cr}}{Z_t} - f_{pc} \tag{1}$$

in which P_{cr} and M_{cr} are the experimentally observed load and moment on the segment at the time of cracking (determined to be consistent with the previously described intersection point for the critical face), A_t and Z_t are the appropriate transformed area and section modulus, and f_{pc} is the prestressing stress in the concrete. f''_t is considered to be the "true" cracking strength of the concrete as exhibited in a wall segment.

The average stress at which cracking is exhibited on a load-strain plot has also been computed as

$$f_{to} = \bar{P}_{cr}/A_t - f_{pc} \tag{2}$$

where $\bar{P}_{cr}$ is the load at the intersection point of a plot of P against the average of the strains on both faces of the specimen. The values of f'_t, f'_c and f''_t and f_{to} determined for nine specimens are tabulated in Table 1. Various ratios of these values are also shown in this table together with mean values and standard deviations.

It should be noted that for the tabulated specimens the average values are

$$f'_t = 6.15\sqrt{f'_c} \tag{3}$$

$$f''_t = 3.65\sqrt{f'_c} \tag{4}$$

$$f''_t = 0.6\, f'_t \tag{5}$$

This indicates that the "true" cracking strength in the wall segment tests had a mean value of only 60% of that which would be predicted from a split cylinder test. Ref. 2 attributes this discrepancy to volume and rate effects.

4. Determination of Degrading Stiffness

In an attempt to determine an effective uniaxial post-cracking tensile curve for concrete, suitable for use with a biaxial elastic-plastic concrete constitutive relationship [3,4], the following procedure was used. The "effective stress" in the concrete was determined in each direction from the test results as

$$\sigma_{c1}A_{c1} = P_1 - E_{s1}A_{s1}(\varepsilon_1 + \varepsilon_{si1}) - E_{p1}A_{p1}(\varepsilon_1 + \varepsilon_{pe1}) \tag{6a}$$

$$\sigma_{c2}A_{c2} = P_2 - E_{s2}A_{s2}(\varepsilon_2 + \varepsilon_{si2}) - E_{p2}A_{p2}(\varepsilon_2 + \varepsilon_{pe2}) \tag{6b}$$

in which σ indicates stress, P indicates load, E indicates modulus of elasticity, A indicates area, and ε indicates strain. The subscripts c, s, and p stand for concrete, steel, and prestressing steel, respectively. Subscripts 1 and 2 indicate directions. ε_{pe} and ε_{si} are the effective strain in the prestressing and reinforcing steel, respectively, prior to application of external load, while ε_1 and ε_2 are measured average strains including both faces of the specimen.

Determine the elastic strains ε_1^E and ε_2^E as

$$\begin{Bmatrix} \varepsilon_1^E \\ \varepsilon_2^E \end{Bmatrix} = \frac{1}{E_c}\begin{bmatrix} 1 & -\nu_c \\ -\nu_c & 1 \end{bmatrix}\begin{Bmatrix} \sigma_{c1} \\ \sigma_{c2} \end{Bmatrix} \tag{7}$$

where E_c and ν_c are the concrete modulus and Poisson's ratio, respectively. Define the plastic strain components ε_1^P and ε_2^P as

$$\begin{Bmatrix} \varepsilon_1^P \\ \varepsilon_2^P \end{Bmatrix} = \begin{Bmatrix} \varepsilon_1 \\ \varepsilon_2 \end{Bmatrix} - \begin{Bmatrix} \varepsilon_1^E \\ \varepsilon_2^E \end{Bmatrix} \tag{8}$$

Define the equivalent plastic strain $\bar{\varepsilon}^P$ as

$$\bar{\varepsilon}^P = \sqrt{\langle\varepsilon^P\rangle\{\varepsilon^P\}} \tag{9}$$

The equivalent total uniaxial strain ε was then defined as

$$\varepsilon = \frac{\sigma}{E_c} + \bar{\varepsilon}^P \tag{10}$$

where σ is the σ_c stress from eqs. 6 in the direction that first cracks. Plotting the σ and ε values of eq. 10 produces a curve which the writers considered to be an adequate representation of an effective uniaxial stress-strain curve for use with the plasticity theory of Ref. 3.

The effective tensile stress-strain curves for the prestressed segments (only), determined as above and nondimensionalized by the f_{to} value of Table 1, are shown in Fig. 4. There is considerable scatter. This is not surprising considering the difficulty of carrying out such tests, the variability of the concrete and the variation in size, spacing and cover on the mild steel reinforcement. Nevertheless, the general trend of a gradual post-cracking softening in the effective uniaxial stress-strain curve is clearly evident. Three approximations to this spectrum of curves are also shown on Fig. 4. An exponential regression analysis for Specimens 1, 3, 5 and 8 is shown as Curve A. Two simple "lower bound" approximations are designated as the "first and second approximations". The effectiveness of these curves in simulating the behaviour of various segments can now be determined by using them as input for a computer analysis of biaxially loaded segments. The results from such simulations are discussed in the following.

5. Simulations of Experimental Behavior

If the approximate uniaxial tensile stress-strain curves shown in Fig. 4 are to have validity, an analytical model of a segment test should produce results which agree with experimental observations when the aforementioned stress-strain properties are input to the analysis. If such correlation can be obtained it serves to verify the effectiveness of the material properties for use with the particular analytical method.

The material properties derived herein have been used in conjunction with the BOSOR5 program [5,6] in order to simulate segment behavior. The material model is an elastic-plastic model which has been described in Refs. 3 and 4. BOSOR5 permits the modelling of a segment by identifying layers of different materials through the thickness. A typical model of a wall segment is shown in Fig. 5.

Analyses were carried out for all segments. The value of f_t'' was taken to be 0.6 f_t' as determined by the mean value on Table 1. Comparison between BOSOR5 analyses and experiment observations for Segments 1 and 3 are shown on Figs. 6 and 7. These specimens had external load ratios of 1:2 and 1:1, respectively, in the two orthogonal directions. It can be seen that the agreement between predicted and experimental average strains in the direction of maximum strain is excellent for both specimens. However, although the minor strain for Segment 3 is also well represented, that for Segment 1 is underestimated. Comparisons between measured and predicted results for the remainder of the specimens are contained in Ref. 2. Although the correspondence between predicted and observed results is not as good for some specimens as that shown in Figs. 6 and 7, it is sufficiently good to establish the technique as a reliable tool for predicting average maximum strains in thin-walled tension structures. It has, therefore, been used in the analysis of full-scale structures and an example of comparison between predicted and experimental results for a more complex structure is contained in Ref. 7.

It can be demonstrated that the response predicted for a segment is sensitive to the value of f_t'' used in the analysis but is relatively insensitive to the shape of the post-cracking degrading stress-strain relationship. Thus the predictions are effectively the same for both of the approximate curves indicated in Fig. 4. However, the first approximation is more likely to lead to numerical instabilities in the solution after yielding of the reinforcing steel.

6. Summary and Conclusions

A set of experimental tests to determine the response of prestressed concrete wall segments has been described. Analysis of the results indicates that cracking in these segments is initiated at a considerably lower stress than would be indicated from split cylinder tensile tests. Shapes for uniaxial degrading tensile stress-strain curves have been recommended. It has been demonstrated that these concrete properties permit an excellent prediction of the deformations arising in prestressed concrete wall segments when used with an elastic-plastic analysis program, such as BOSOR5.

A word of caution is, however, in order. On the basis of two nonprestressed segments that were included in the test series it appears that reinforced concrete exhibits a significantly lower tensile strength and a somewhat more rapid degradation of stiffness than the prestressed segments discussed herein.

7. Acknowledgements

The work on which this paper is based was sponsored by the Atomic Energy Control Board of Canada, Ottawa, Canada, K1P 5S9.

References

/1/ Rizkalla, S., MacGregor, J.G., Chitnuyanondh, L., Wong, C., and Simmonds, S.H., "Response of Models of Segments from the Walls of Containment Vessels - Presentation of Test Data," Structural Engineering Report, Dept. of Civil Engineering, University of Alberta, Edmonton, Alberta, 1979.

/2/ Chitnuyanondh, L., Rizkalla, S., Murray, D.W., and MacGregor, J.G., "An Effective Uniaxial Stress-Strain Relationship for Prestressed Concrete", Structural Engineering Report No. 74, Department of Civil Engineering, University of Alberta, Edmonton, Alberta, February 1979.

/3/ Murray, D.W., Chitnuyanondh, L., Rijub-Agha, K.Y., and Wong, C., "A Concrete Plasticity Theory for Biaxial Stress Analysis", submitted to the Journal of the Engineering Mechanics Division, ASCE, August, 1978.

/4/ Murray, D.W., Chitnuyanondh, L., Wong, C., and Rijub-Agha, K.Y., "Inelastic Analysis of Prestressed Concrete Secondary Containments," Structural Engineering Report No. 67, Department of Civil Engineering, University of Alberta, Edmonton, Alberta, July 1978.

/5/ Bushnell, D., "BOSOR5 - A Computer Program for Buckling of Elastic-Plastic Complex Shells of Revolution Including Large Deflections and Creep",
(a) "Vol. 1: User's Manual, Input Data", LMSC D407166, Dec. 1974.
(b) "Vol. 3: Theory and Comparisons with Tests", LMSC D407168, Dec. 1974.
Lockheed Missiles and Space Company, Sunnyvale, California.

/6/ Bushnell, D., "A Strategy for the Solution of Problems Involving Large Deflections, Plasticity and Creep", International Journal for Numerical Methods in Engineering, Vol. 11, 1977, 683-708.

/7/ Rizkalla, S., Simmonds, H., and MacGregor, J.G., "A Test of a Model of a Thin-Walled Prestressed Concrete Secondary Containment Structure," Transactions of SMiRT5, Paper No. J 4/2, Berlin, Aug. 1979.

Table 1. Measured and Computed Strengths of Concrete of Wall Segments

1	2	3	4	5	6	7	8	9	10	11
Specimen Number	Prestressing	Cylinder Strengths, psi			Estimated[1] Cracking Load, kip	Computed tensile strength, psi[2]		$\frac{f''_t}{f'_t}$	$\frac{f''_t}{\sqrt{f'_c}}$	Mean Strain at First Crack $\times 10^{-6}$
		f'_t	f'_c	$f'_c/\sqrt{f'_c}$		f''_t	f_{to}			
[illegible]	none	536	5590	7.17	60 (1)	256	171	0.48	3.42	80
7[4]	none	312	3290	5.44	75.1(1)	168	142	0.54	2.93	300
5	1 dir.	444	5690	5.89	255.5(2)	389	374	0.88	5.16	170
6	1 dir.	325	4540	4.81	185.0(2)	223	139	0.69	3.31	160
[illegible]	2 dir.	426	5690	5.63	206.8(2)	229	193	0.54	3.04	190
1	2 dir.	490	5090	6.87	300.0(1)	307	225	0.63	4.30	370
2	2 dir.	436	4460	6.53	287.0(1)	174	136	0.40	2.61	90
8	2 dir.	424	4920	6.05	350.0(1)	321	308	0.76	4.58	390
9	2 dir.	437	3920	6.98	300.0(1)	221	176	0.51	3.53	—
				6.15	= MEAN =			0.60	3.65	220[3]
				0.79	= STANDARD DEVIATION =			0.15	0.85	120
				0.13	= COEFF. OF VARIATION =			0.25	0.23	0.55

1. The number in parentheses denotes the direction which cracks first appeared, i.e. (1) refers to horizontal cracks (due to vertical loads), whereas (2) refers to vertical cracks (due to horizontal loads).
2. f''_t and f_{to} are computed with and without bending moments, respectively.
3. The average in col. 11 is computed without segment 9 which has spliced rebars.
4. Specimen 7 contains 2 batches of concrete, the strengths in columns 3 and 4 are for the face on which the cracks started.

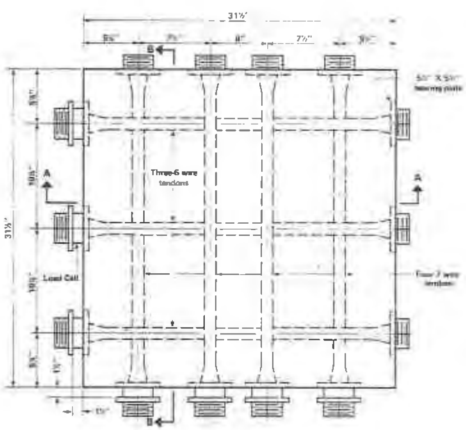

Figure 1. Segment Test Specimen Dimensions

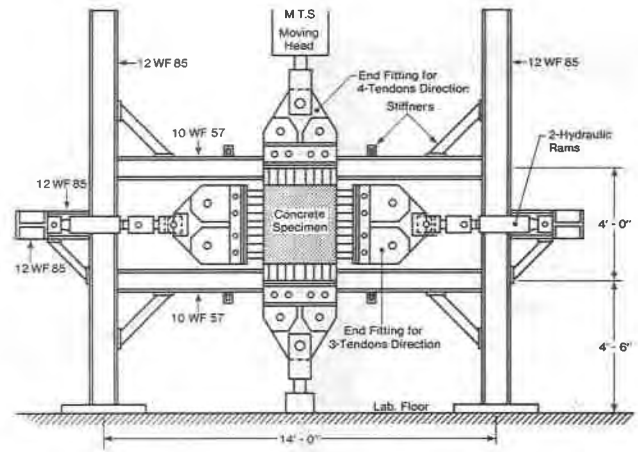

Figure 2. Test Set-Up

Figure 3. Specimen 2 After Testing

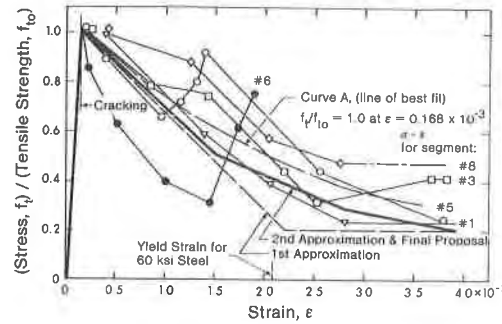

Figure 4. Uniaxial Tensile Stress-Strain Curves

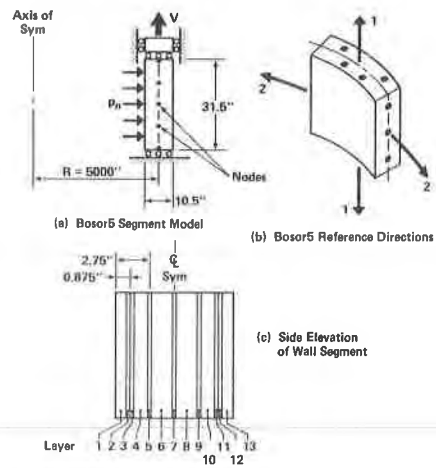

Layers	Thickness	Material*
1,13	0.8401	1
4,10	1.8268	1
6,8	2.4696	1
2,12	0.0349	2
3,11	0.0349	3
5,9	0.0266	4
7	0.0342	5

(d) Details of Layers

Figure 5. BOSOR5 Model of Specimen

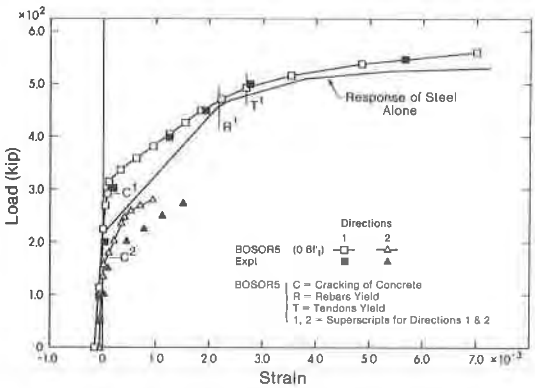

Figure 6. Load-Strain Response: Segment 1

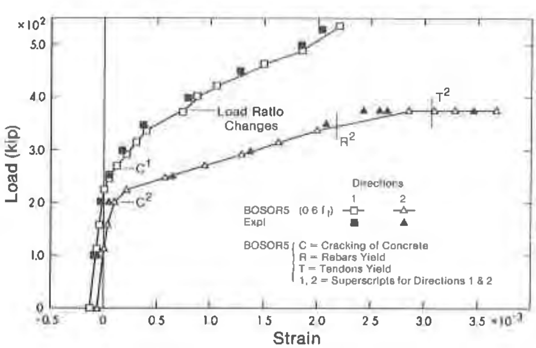

Figure 7. Load-Strain Response: Segment 3